

A Hand Motion Controller Allowing for Control the Computer Models and Peripherals*

JAKUB BERNAT, SEBASTIAN BUKOWIECKI, JAKUB KOLOTA and SŁAWOMIR STĘPIEŃ

Chair of Computer Engineering, Poznan University of Technology, Piotrowo 3a, 60-965 Poznań, Poland.

E-mail: Jakub.Kolota@put.poznan.pl

Recent years have brought important changes in engineering education, especially in electrical and computer engineering. Along with new equipment and modern electronics, there are new opportunities in the automation control. This paper presents a hand motion controller, which measures the orientation of the upper limb of a man in three dimensional space. The design assumes the use of microcontrollers from Texas Instruments, which will be responsible for communication between specific modules. It assumed the usage of two types of communication UART (Universal Asynchronous Receiver and Transmitter) and I2C (called Inter-Integrated Circuit). Microcontrollers will also be responsible for monitoring the voltage and simple calculations. The entire system has been sown in the glove acting module possible to connect to different devices, and communicating through the I2C bus with the master device. In order to visualize the controller a hand model was developed in an environment of OpenGL and 3ds Max. Subsequently, the control program which is responsible for calculating the rotation matrix, and the calculation (using data from the matrix) of degrees of freedom associated with the forearm and the arm, was implemented. This is a broader issue related to the large number of calculations which are not capable of microcontrollers (requires a large computational power), that was the reason which extorted the computer's calculations communicated with the controller wirelessly by Bluetooth. In order to present the results, a physical manipulator, which mimics the trajectory of hand movement, was connected to a personal computer. Presented system is used on the experimental laboratory education on Chair of Computing Engineering at Poznan University of Technology in Poland. The objective is to present remote laboratory kits for teaching and learning some aspects of control systems. Additionally, the effectiveness of the platforms in educating students is discussed.

Keywords: hand motion controller; three-axis gyroscopes model; wireless navigation controller; rotation matrix

1. Introduction

Laboratories, which are found in all engineering and science programs, are an essential part of the education experience. They bring the course theory alive so students can see how unexpected events and natural phenomena affect real-world measurements and control algorithms [1–4, 12]. The education of Automatics and Robotics through computer-based environments has dynamically increased and has opened a variety of new avenues and methodologies for enhancing the experience of learning. It is very important to present knowledge in interesting form, especially in the engineering faculties [1, 2, 9, 10, 12, 15]. This paper presents the new approach to high-level device for natural human-computer interfaces. The authors' goal was to construct a compact hand controller that could provide large workspace with wireless communication with personal computer.

The development and progress of various types of machinery and robots entails the need for expansion of knowledge that enables an intuitive control. In most cases, traditional hardware controllers are not sufficient. Consumers want to have a controller with a short reaction time, which can directly control a device or process in an intuitive way, very often with the wireless transmission of control signals. The authors have proposed a controller which can control various devices connected to the computer through human upper limb motion. This solution reduces response time to a minimum and at the same time allows for full and easy control with the operator's hand in wireless way. Thesis is the design and construction of devices to measure the location of all human upper limb in three dimensions. This is possible through the use of microcontrollers, gyroscopes and flex sensors with Bluetooth communication interface and OpenGL visualization [6, 15].

The presented device can be used to control various types of robots and automation processes. Through the use of rotation matrices, the controller is particularly suitable for handling arms with many degrees of freedom transforming positions and laying hands on the data required for controlling the machines [8]. There are many devices that allow to control the process by hand, but not many devices can do this with the entire upper limb. This approach opens new possibilities for the usage of industrial robots.

2. The Construction of the hand motion controller

The controller has five degrees of freedom using the reading from the two three-axis velocity gyroscopes. They indicate the angular velocity of rotation of the body in all three axes of the coordinate system to which they are attached [5]. Each of the five degrees of freedom is determined by reading six angles. PmodGyro system was used, which contains sensors L3G4200D (Fig. 1).

The sensor has low power consumption and has a built-in communication. It was made in MEMS (Micro Electro-Mechanical System) technology by STMicroelectronics. The main advantages of the layout are [5]:

- standard SPI and I2C interface
- three possible working definition: 250/500/2000dps
- two pins responsible for the interruption
- built-in signal filters
- built-in temperature sensor
- normal and sleep operating modes are available
- built-in FIFO queue
- high resistance to shocks and adverse temperature
- wide power supply range from 2.4V to 3.6V.

Gyroscopes of this type are usually used in the following sections: traffic control (devices controlled by humans), robotics, various types of GPS navigation systems [5].

The study used MSP430 family of microcontrollers from Texas Instruments [6]. They are characterized by low power voltage, additionally; the price of microcontrollers is maintained at low levels.

These microcontrollers are built for 16-bit processors. These microcontrollers are used in wireless devices, battery powered. The MSP430 has six different low-power modes. Therefore, it is possible to disable the CPU while the peripherals perform a task in which the processor is not needed. In addition, it is possible to return to normal operation, the microcontroller in less than 1 microsecond. These devices depending on the application have a different configuration of peripherals (internal oscillator, timers with PWM, watchdog, USART, USI, ADC 10/12/14/16-bit, comparators, 12-bit DAC, LCD driver, etc.) [6]. Microcontrollers are adapted to programming using assembly language and C language being programmed via JTAG. The described hand motion controller uses two microcontrollers MSP430G2231. The StarterKit MSP430 LaunchPad has been used for programming and testing the microcontroller (Fig. 2).

The device sends its data to a computer in a wireless interface. KAmoDBTM222 module was used to support Bluetooth communication and communicates through URAT with an external devices. External device such as a computer is configured to communicate with the module by setting the appropriate parameters (baud rate: 19200 bps, data bit: 8, parity: none, stop bit: 1, flow control: none).

The glove module is a separate part of the motion controller, which communicates via I2C protocol. This module consists of six sensors that respond to the fingers and wrist flexion (Fig. 3). These sensors operate on the principle of resistance changes according to their curvature. Resistance of the sensors is converted to a voltage by using a dedicated system. The output voltage is then measured by a microcontroller, scaled and sent to a device that communicates with it. To measure the change in resistance properly, the operational amplifier was used. Resistance of the sensors in their nominal position is about 10 k Ω , so subtraction should be used and the corresponding strengthening of the resulting voltage.

Table 1 presents the measurements of the limit values of resistors (minimum value for straight position and

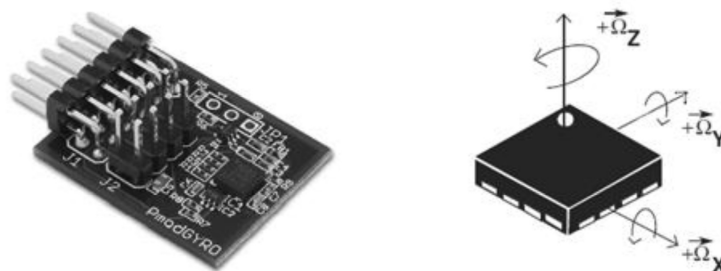


Fig. 1. A view of PmodGyro control module and description of the axis of the system [10].

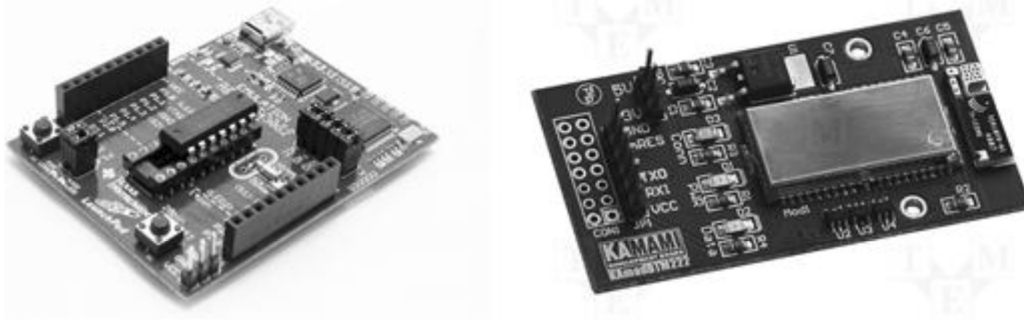


Fig. 2. A view of MSP430 LaunchPad (left) and KAmobBTM222 module (right) [10].

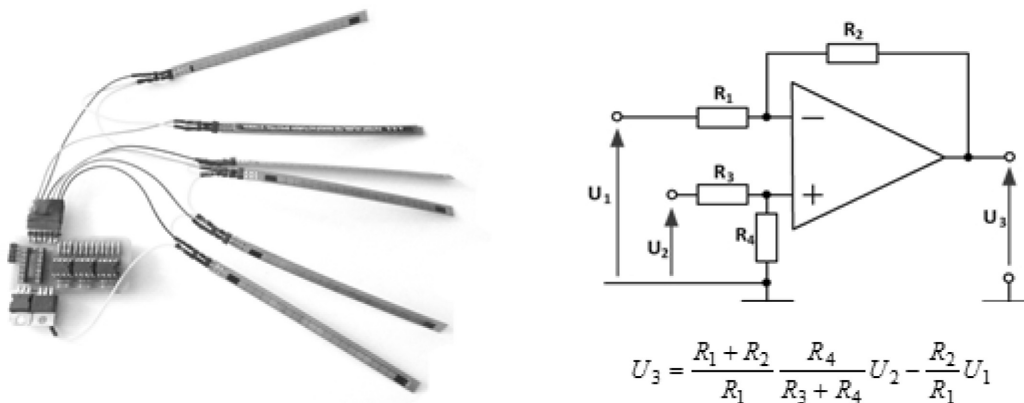


Fig. 3. A view of flex sensors module and diagram of the amplifier electronics.

$$U_3 = \frac{R_1 + R_2}{R_1} \frac{R_4}{R_3 + R_4} U_2 - \frac{R_2}{R_1} U_1$$

Table 1. The measurements of the limit values of each flex resistors

Number of resistor	Value of the minimum resistance [kΩ]	Value of the maximum resistance [kΩ]
1	12	19.5
2	12	19
3	11.9	19.5
4	10.4	19
5	11	19.8
6	8.6	13.8

maximum value for curved position). The value of the resistor nr 6 was measured on the wrist, so its value significantly differed from the others. For this resistor system was set with different parameters in comparison with the others.

To properly examine the resistance value, it was proposed following the layout in Fig. 4. where:

U_1 – 1.8V fixed voltage reference, U_2 – AC voltage depending on resistance value R_x , U_3 – the entire system power supply voltage 3.3V, U_4 – the voltage across the resistor R_x , U_{wy} – output voltage, served on a microcontroller, R_1 and R_2 – resistors which values are searched, R_x – variable resistance sensor.

The microcontroller was programmed to measure the voltage range from 0V to 1.5V. Resistance values should be adjusted—change of the resistance R_x should cause a change of the output voltage in the desired range. After the necessary calculation, the level of the resistance R_1 and R_2 was determined adequately 7 kΩ and 17kΩ. For the flex sensor mounted on the wrist (resistor nr 6), the resistance levels are $R_1 = 4$ kΩ and $R_2 = 13$ kΩ.

The device is built on a universal PCB module. The system contains six systems described above (for each sensor), microcontroller, the voltage stabilizer and the outputs for to the sensors, power supply and communication. Five flex sensors are attached to the respective fingers, and one to the wrist. The whole was enclosed in a glove comfortable to set up and use.

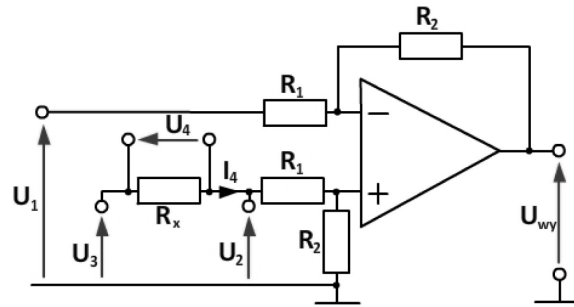


Fig. 4. A view of circuit diagram for measuring the resistance values.

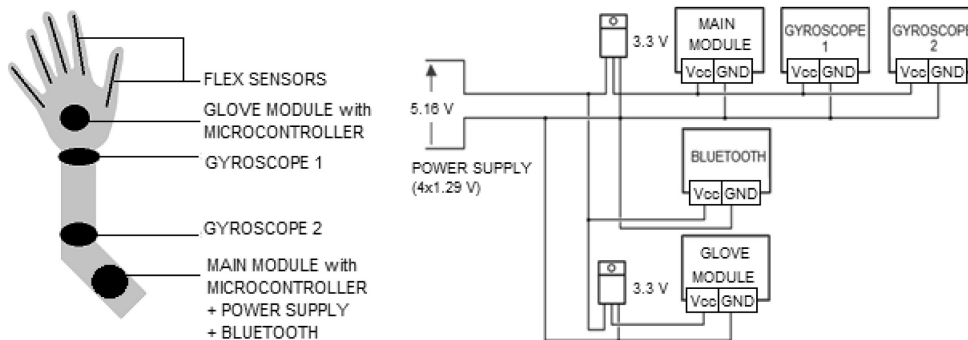


Fig. 5. Construction view and power scheme of the hand motion controller.

The main part of the hand motion controller is responsible for communication with the modules and their respective power. It consists of a microcontroller and power supply system (four AA batteries and a voltage regulator 3.3V). Then the other modules have been added: two PmodGyro (gyroscopes), KAmoBTM222 (Bluetooth) and a module of the glove, described above. This device collects information from the gyroscopes and the module glove and then sends it via Bluetooth to an external device. This section communicates with the other modules only when Bluetooth returns the information that was successfully combined with an external device.

The main unit is powered by four AA batteries that are connected in series. Every charged battery has 1.29 [V] power supply system. Serial connection makes the obtained voltage value of 5.16V. This voltage is suitable for the Bluetooth system, but it is too high for the other components. For this reason, it was decided to use a voltage stabilizer that will keep the output constant voltage value 3.3V. The system power scheme is depicted in Fig. 5.

3. The kinematic model of the hand motion controller

Each of the two gyroscopes has referred to its rotation matrix. Both arrays during initialization of the device have a value:

$$M_1 = M_2 = \begin{bmatrix} 1 & 0 & 0 \\ 0 & 1 & 0 \\ 0 & 0 & 1 \end{bmatrix} \tag{1}$$

After each reading data from the gyroscope these matrices are multiplied by the elementary rotation matrices relative to the individual axis. This is done in order to get the gyroscope rotation matrix in the global coordinate system. The rotation matrix around the X axis by an angle α :

$$rotX = \begin{bmatrix} 1 & 0 & 0 \\ 0 & \cos \alpha & -\sin \alpha \\ 0 & \sin \alpha & \cos \alpha \end{bmatrix} \tag{2}$$

The rotation matrix around the Y axis by an angle β :

$$\text{rot}Y = \begin{bmatrix} \cos \beta & 0 & \sin \beta \\ 0 & 1 & 0 \\ -\sin \beta & 0 & \cos \beta \end{bmatrix} \quad (3)$$

The rotation matrix around the Z axis by an angle γ :

$$\text{rot}Z = \begin{bmatrix} \cos \gamma & -\sin \gamma & 0 \\ \sin \gamma & \cos \gamma & 0 \\ 0 & 0 & 1 \end{bmatrix} \quad (4)$$

To obtain the rotation matrix around the whole gyroscope, multiplication of the rotation matrix should be done for each new reading of angles:

$$M_x = M_{x-1} * \text{Rot}H \quad (5)$$

where:

M_x – a rotation matrix of the gyroscope for which the data are read (x takes the value 1 or 2), M_{x-1} – the previous value of the rotation matrix for the gyroscope, $\text{Rot}H$ – one of three elementary rotation dependent on the axis around which the actual reading is performed (H is one of the three axes: X, Y or Z).

Shoulder joint is the main joint which rotates the entire human upper limb. It is a spherical joint which connects the upper limb with the limb shoulders. Construction of the joint makes it appear in three degrees of freedom associated with the rotation of the arm around the three axes of the coordinate system X, Y, Z. Gyroscope is attached to the arm, so it is possible to calculate the angles of rotation about the shoulder joint. The global coordinate system associated with the visualization of the arm has been suggested as in Fig. 6.

Submission of a rotation matrix corresponds to three degrees of freedom of the shoulder:

$$M_1 = \text{Rot}Y * \text{Rot}Z * \text{Rot}X \quad (6)$$

Presented a rotation matrix facilitates the understanding of the angles α, β, γ . The angle α associated with the X axis is responsible for the twist of the arm. The angle β associated with the Y axis is responsible for moving the arm to the side. And the angle γ associated with the Z axis is responsible for raising and leaving the arm.

The above equation is transformed in such a way to get the angles α, β, γ . The first step is calculates the $\text{Rot}Y * \text{Rot}Z$:

$$\text{Rot}Y * \text{Rot}Z = \begin{bmatrix} \cos \beta & 0 & \sin \beta \\ 0 & 1 & 0 \\ -\sin \beta & 0 & \cos \beta \end{bmatrix} \begin{bmatrix} \cos \gamma & -\sin \gamma & 0 \\ \sin \gamma & \cos \gamma & 0 \\ 0 & 0 & 1 \end{bmatrix} = \begin{bmatrix} \cos \beta \cos \gamma & -\cos \beta \sin \gamma & \sin \beta \\ \sin \gamma & \cos \gamma & 0 \\ -\sin \beta \cos \gamma & \sin \beta \sin \gamma & \cos \beta \end{bmatrix} \quad (7)$$



Fig. 6. Global coordinate system used in the model.

Following this:

$$[RotY * RotZ] * RotX = \begin{bmatrix} \cos \beta \cos \gamma & -\cos \beta \sin \gamma & \sin \beta \\ \sin \gamma & \cos \gamma & 0 \\ -\sin \beta \cos \gamma & \sin \beta \sin \gamma & \cos \beta \end{bmatrix} \begin{bmatrix} 1 & 0 & 0 \\ 0 & \cos \alpha & -\sin \alpha \\ 0 & \sin \alpha & \cos \alpha \end{bmatrix} \quad (8)$$

$$M_1 = RotY * RotZ * RotX = \begin{bmatrix} \cos \beta \cos \gamma & -\cos \beta \sin \gamma \cos \alpha + \sin \beta \sin \alpha & \cos \beta \sin \gamma \sin \alpha + \sin \beta \cos \alpha \\ \sin \gamma & \cos \gamma \cos \alpha & -\cos \gamma \sin \alpha \\ -\sin \beta \cos \gamma & \sin \beta \sin \gamma \cos \alpha + \cos \beta \sin \alpha & -\sin \beta \sin \gamma \sin \alpha + \cos \beta \cos \alpha \end{bmatrix} \quad (9)$$

Assuming the first gyroscope rotation matrix (measured and known in real time):

$$M_1 = \begin{bmatrix} m_{1,11} & m_{1,12} & m_{1,13} \\ m_{1,21} & m_{1,22} & m_{1,23} \\ m_{1,31} & m_{1,32} & m_{1,33} \end{bmatrix} \quad (10)$$

It is possible to compare the matrixes to each other and find the unknowns:

$$\begin{bmatrix} m_{1,11} & m_{1,12} & m_{1,13} \\ m_{1,21} & m_{1,22} & m_{1,23} \\ m_{1,31} & m_{1,32} & m_{1,33} \end{bmatrix} = \begin{bmatrix} \cos \beta \cos \gamma & -\cos \beta \sin \gamma \cos \alpha + \sin \beta \sin \alpha & \cos \beta \sin \gamma \sin \alpha + \sin \beta \cos \alpha \\ \sin \gamma & \cos \gamma \cos \alpha & -\cos \gamma \sin \alpha \\ -\sin \beta \cos \gamma & \sin \beta \sin \gamma \cos \alpha + \cos \beta \sin \alpha & -\sin \beta \sin \gamma \sin \alpha + \cos \beta \cos \alpha \end{bmatrix} \quad (11)$$

Subsequently:

$$\frac{-\sin \beta \cos \gamma}{\cos \beta \cos \gamma} = \frac{m_{1,31}}{m_{1,11}} \quad (12)$$

Therefore:

$$\frac{\sin \beta}{\cos \beta} = \frac{-m_{1,31}}{m_{1,11}} \quad (13)$$

Then β angle can be calculated using *atan2* function:

$$\beta = a \tan 2(-m_{1,31}, m_{1,11}) \quad (14)$$

Other angles can be calculated analogously:

$$\alpha = a \tan 2(-m_{1,23}, m_{1,22}) \quad (15)$$

Since the angle β has been calculated, it can be used to calculate the angle γ :

$$\gamma = a \tan 2(-m_{1,21}, \frac{m_{1,11}}{\cos \beta}) \quad (16)$$

This way lets us calculate three angles associated with three degrees of freedom of the shoulder.

The next two degrees of freedom are related to the forearm (Fig. 7). The first is the elbow joint and the second is the ability to twist the forearm. The first problem to be solved is how different position of the second gyroscope relates to the first one. Angle values received from the second gyroscope should be assigned to appropriate axis of the first gyroscope.

None of the axis of the second gyroscope does not coincide with the axis of the first gyroscope in the initial position of the controller. M_2 matrix as well as the M_1 matrix points out the rotation of the gyroscope in the global coordinate system. Therefore, in order to find the degrees of freedom associated with the orientation of the forearm, the first gyroscope should be considered.

$$M_2 = M_1 * M_B \quad (17)$$

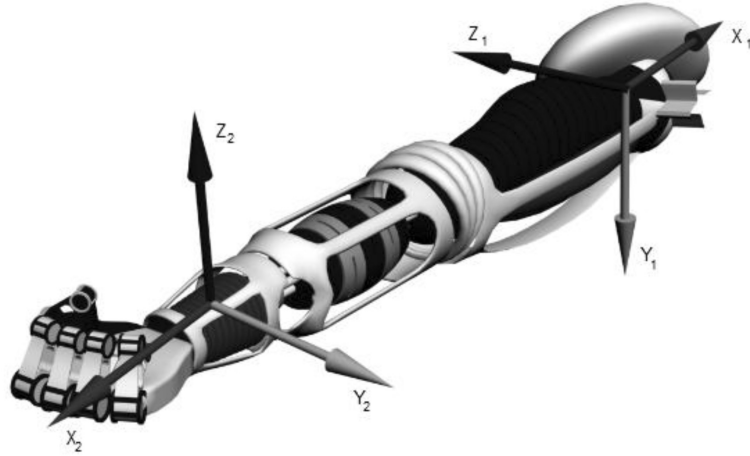


Fig. 7. Internal coordinate systems of two gyrosopes.

where M_B is a matrix describing rotation between the system of the first and second gyrosopes. It can be defined as:

$$M_B = M_{1-1} * M_2 \quad (18)$$

Matrices M_1 and M_2 are known, so inverse matrix M_{1-1} can be determined.

$$M_{1-1} = \frac{1}{\det(M_1)} D^T \quad (19)$$

where D^T is a matrix, which is calculated as follows:

$$d_{11} = (-1)1 + 1 \det \begin{pmatrix} m_{1,22} & m_{1,23} \\ m_{1,32} & m_{1,33} \end{pmatrix} = m_{1,22}m_{1,33} - m_{1,23}m_{1,32}$$

$$\bullet$$

$$\bullet$$

$$\bullet$$

$$d_{33} = (-1)3 + 3 \det \begin{pmatrix} m_{1,11} & m_{1,12} \\ m_{1,21} & m_{1,22} \end{pmatrix} = m_{1,11}m_{1,22} - m_{1,12}m_{1,21} \quad (20)$$

The next step is to determine the rotation matrix which describes M_B . The first rotation is associated with an elbow joint. This rotation matrix occurs around the axis Z . The second rotation matrix results from the possibility of turning the forearm and it is rotation around the axis X . Therefore M_B rotation matrix is defined as:

$$M_B = RotZ * RotX \quad (21)$$

Following this:

$$RotZ * RotX = \begin{bmatrix} \cos \gamma & -\sin \gamma & 0 \\ \sin \gamma & \cos \gamma & 0 \\ 0 & 0 & 1 \end{bmatrix} \begin{bmatrix} 1 & 0 & 0 \\ 0 & \cos \alpha & -\sin \alpha \\ 0 & \sin \alpha & \cos \alpha \end{bmatrix} = \begin{bmatrix} \cos \gamma & -\sin \gamma \cos \alpha & \sin \gamma \sin \alpha \\ \sin \gamma & \cos \gamma \cos \alpha & -\cos \gamma \sin \alpha \\ 0 & \sin \alpha & \cos \alpha \end{bmatrix} \quad (22)$$

To calculate the angles γ and α , compare:

$$\begin{bmatrix} \cos \gamma & -\sin \gamma \cos \alpha & \sin \gamma \sin \alpha \\ \sin \gamma & \cos \gamma \cos \alpha & -\cos \gamma \sin \alpha \\ 0 & \sin \alpha & \cos \alpha \end{bmatrix} = \frac{1}{\det(M_1)} \begin{bmatrix} d_{11} & d_{21} & d_{31} \\ d_{12} & d_{22} & d_{32} \\ d_{13} & d_{23} & d_{33} \end{bmatrix} \begin{bmatrix} m_{2,11} & m_{2,12} & m_{2,13} \\ m_{2,21} & m_{2,22} & m_{2,23} \\ m_{2,31} & m_{2,32} & m_{2,33} \end{bmatrix} \quad (23)$$

To calculate the angles γ and α is sufficient to calculate the following expression:

$$\cos \gamma = \frac{1}{\det(M_1)} [m_{2,11}d_{11} + m_{2,21}d_{21} + m_{2,31}d_{31}] \quad (24)$$

$$\sin \gamma = \frac{1}{\det(M_1)} [m_{2,11}d_{12} + m_{2,21}d_{22} + m_{2,31}d_{32}] \quad (25)$$

$$\sin \alpha = \frac{1}{\det(M_1)} [m_{2,12}d_{13} + m_{2,22}d_{23} + m_{2,32}d_{33}] \quad (26)$$

$$\cos \alpha = \frac{1}{\det(M_1)} [m_{2,13}d_{13} + m_{2,23}d_{23} + m_{2,33}d_{33}] \quad (27)$$

Therefore:

$$\frac{\sin \gamma}{\cos \gamma} = \frac{m_{2,11}d_{12} + m_{2,21}d_{22} + m_{2,31}d_{32}}{m_{2,11}d_{11} + m_{2,21}d_{21} + m_{2,31}d_{31}} \quad (28)$$

$$\frac{\sin \alpha}{\cos \alpha} = \frac{m_{2,12}d_{13} + m_{2,22}d_{23} + m_{2,32}d_{33}}{m_{2,13}d_{13} + m_{2,23}d_{23} + m_{2,33}d_{33}} \quad (29)$$

And finally:

$$\gamma = a \tan 2(m_{2,11}(-m_{1,21}m_{1,33} + m_{1,23}m_{1,31}) + m_{2,21}(m_{1,11}m_{1,33} - m_{1,13}m_{1,31}) + m_{2,31}(-m_{1,11}m_{1,23} + m_{1,13}m_{1,21}), \\ m_{2,11}(m_{1,22}m_{1,33} - m_{1,23}m_{1,32}) + m_{2,21}(-m_{1,12}m_{1,33} + m_{1,13}m_{1,32}) + m_{2,31}(m_{1,12}m_{1,23} - m_{1,13}m_{1,22})) \quad (30)$$

$$\alpha = a \tan 2(m_{2,12}(m_{1,21}m_{1,32} - m_{1,22}m_{1,31}) + m_{2,22}(-m_{1,11}m_{1,32} + m_{1,12}m_{1,31}) + m_{2,32}(m_{1,11}m_{1,22} - m_{1,12}m_{1,21}), \\ m_{2,13}(m_{1,21}m_{1,32} - m_{1,22}m_{1,31}) + m_{2,23}(-m_{1,11}m_{1,32} + m_{1,12}m_{1,31}) + m_{2,33}(m_{1,11}m_{1,22} - m_{1,12}m_{1,21})) \quad (31)$$

The above method lets us designate are five angles associated with five degrees of freedom.

4. The example of using the hand motion controller and conclusions

The hand motion controller presented in this paper may have wide range of applications (the industry, mobile machines, medicine, space, building etc.) In order to test its real work, the authors have built an industrial manipulator using ten servomechanisms Dynamixel AX-12 Robotis company [11]. Each servomechanism has a unique id number and all construction is managed by dedicated CM-5 controller (Fig. 8) [12].

The objective was to collect the control signals from the hand motion controller by the personal computer, to visualize graphically the position of the hand (Fig. 9), and to send control commands to the controller CM-5. Consequently, the manipulator reflects the hand movements.

In the field of automation, communication and data visualization technologies play an important role. Without communication is hardly possible to build a complex and sophisticated equipment. There are many ways to communicate, though creating a different type of equipment it is worth comparing the advantages and disadvantages of different types of interfaces, in order to choose the right one for the data exchange [1–3, 7]. Communication technologies used in computers differ in many ways. Wireless communication (e.g. Bluetooth) is usually more advanced technology that uses the physical connection.

Differences also occur at the level of power consumption and speed of data transmission [6].

This paper presents the basic methods and technologies of communication that were used in the construction of the universal hand motion controller. This experience gave very good results and encouraged the authors to expand the work in a similar direction in the future. Presented hand motion controller is utilized

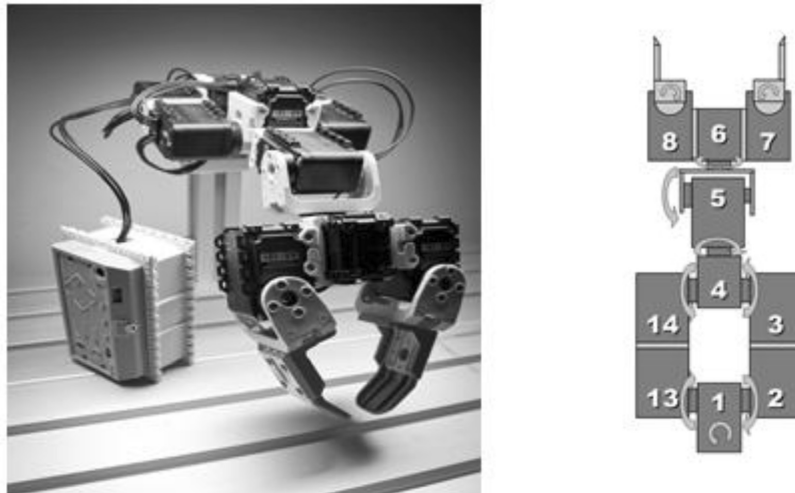


Fig. 8. Construction of the manipulator used in the test device.



Fig. 9. Comparison views of the device and its computer visualization.

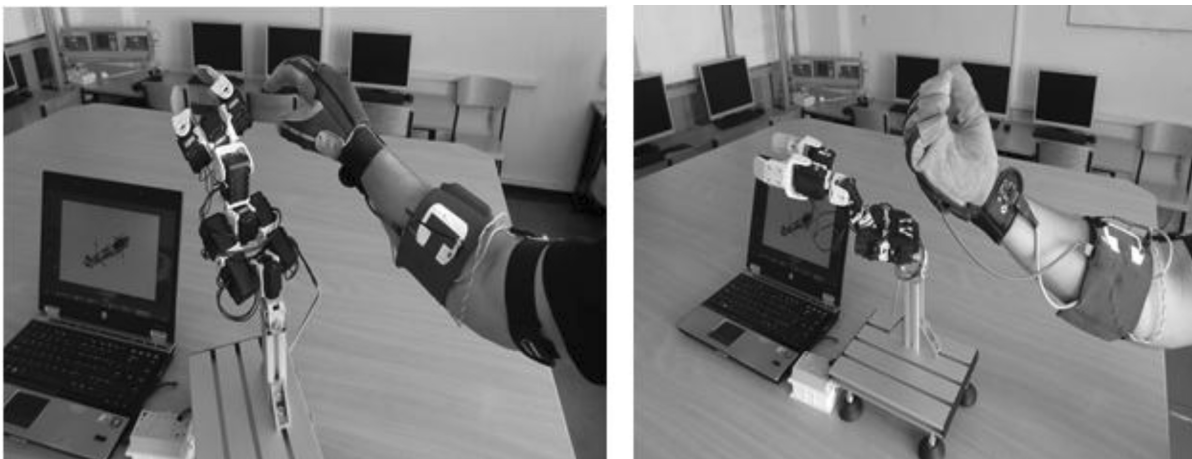


Fig. 10. Verification of the hand motion controller work in the real lab environment.

for practical exercises in the Chair of Computer Engineering specialization during subject “Programming of Industrial Controllers”.

The students are enthusiastic about using the hand motion controller, which replaces the formal devices like mouse and keyboard. The developed device has produced new opportunities for providing more advanced and efficient interfaces to the user. Interesting form of automatic process visualization maintains a high student motivation during the courses and fosters students’ ability to cope with new algorithm problems.

References

1. S. Behnke, J. Mueller and M. Schreiber, *Using Handheld Computers to Control Humanoid Robots*, In Proceedings of 1st International Conference on Dextrous Autonomous Robots and Humanoids (darh2005), Yverdon-les-Bains, Switzerland, May 2005, paper no. 3.2
2. A. W. Bates and G. Poole, *Effective teaching with technology in higher education: Foundations for Success*, San Francisco: Jossey-Bass, 2003.
3. T. A. Bekele, Motivation and Satisfaction in Internet-Supported Learning Environments: A Review. *Educational Technology & Society*, **13**(2), 2010, pp. 116–127.
4. M. Cooper, D. Keating, W. Harwin and K. Dautenhahn, Robots in the classroom: Tools for accessible education. In C. Buhler and H. Knops, *Assistive Technology on the Threshold of the New Millennium* Amsterdam: IOS Press, 1999, pp. 448–452.
5. J. Esfandiyari, R. De Nuccio and G. Xu, *Introduction to MEMS gyroscopes*, STMicroelectronics, Inc., 2010
6. Texas Instruments Corporation *MSP430x2xx Family User's Guide*, <http://www.ti.com>, Accessed 9 June 2012.
7. J. Herrington and R. Oliver, An instructional design framework for authentic learning environments. *Educational Technology Research and Development*, **48**(3), 2006, pp. 23–48.
8. T. Inoue and S. Hirai, *A two-phased object orientation controller on soft finger operations*, International Conference on Intelligent Robots and Systems, 2007, pp. 2528 – 2533
9. D. Ionescu., B. Ionescu, C. Gadea and S. Islam , *A multimodal interaction method that combines gestures and physical game controllers*, Proceedings of 20th International Conference on Computer Communications and Networks (ICCCN), 2011, pp. 1–6
10. J. H. Kim, D. T. Nguyen and K. Tae-Seong, *3-D hand motion tracking and gesture recognition using a data glove*, IEEE International Symposium on Industrial Electronics, 2009, pp. 1013–1018
11. Kamami Development Tools Corporation, <http://www.kamami.pl>, Accessed 16 May 2012.
12. R. Pintrich and D. H. Schunk, *Motivation in education: Theory, research, and applications* (2nd Ed.), New Jersey, USA: Merrill Prentice Hall, 2002.
13. Robotis Corporation *Bioloid User's Guide* and *AX-12 Manual*, <http://www.robotis.com>, Accessed 3 May 2012.
14. J. Stuecker and S. Behnke, *Soccer Behaviors for Humanoid Robots*, Workshop on Humanoid Soccer Robots of the IEEE-RAS International Conference on Humanoid Robots (Humanoids'06), Genoa, Italy, December 2006, pp. 62–70.
15. R. S. Wright, N. Haemel, G. Sellers and B. Lipchak, *OpenGL SuperBible: Comprehensive Tutorial and Reference*, Pearson Education Inc., 2010

Jakub Bernat received the Ph.D. degree in Control Systems from Poznan University of Technology, Poland, in 2011. He is currently working on the control theory and its applications. His main research areas are the adaptive systems, robust control and electromagnetic analysis.

Sebastian Bukowiecki received the M.Sc. degree from Poznan University of Technology, Poland, in 2012. He makes a simulations and analysis of modern communication technologies and interfaces in application to automatics and robotics. He specializes in programming microcontrollers Texas Instruments Company.

Jakub Kolota received the Ph.D. degree from Poznan University of Technology, Poland, in 2009, and the M.Eng. degree from the same University in 2000. Currently, he is a research scientist in the Chair of Computer Engineering in the Informatics Department, Poznan University of Technology, Poland. In 2010 has been honored by the Informatics Department with the award for excellence in teaching. He makes a simulations and analysis of dynamics of electromagnetic devices in application to automatics and robotics. In Ph.D. thesis he described a complex simulation of reluctance stepper motor, represented in 3D space with distributed parameters.

Sławomir Stępień received the M.Eng. degree from Poznan University of Technology, Poland, in 2000, and the Ph.D. degree from the same University in 2005. He is presently a Research Scientist in the Chair of Computer Engineering, Poznan University of Technology, Poland. His research interests include electromagnetic field analysis and synthesis, electrical machines control, identification and optimisation of electromagnetic devices.